



universität
wien

MASTERARBEIT

Titel der Masterarbeit

Lock-in based detection scheme for a hydrogen
beam

Verfasser

Michael Wolf, BSc

angestrebter akademischer Grad

Master of Science (MSc)

Wien, 2013

Studienkennzahl lt. Studienblatt:

A 066 876

Studienrichtung lt. Studienblatt:

Masterstudium Physik

Betreuer:

Hon.-Prof. Dipl.-Phys. Dr. Eberhard Widmann

DANKSAGUNG

Als erstes möchte ich meinem Betreuer danken. Danke Eberhard, dass du mir die Möglichkeit gegeben hast eine Masterarbeit am Stefan-Meyer-Institut zu schreiben.

Daneben gilt mein Dank meinen Kollegen Martin, Martin und Peter mit denen ich intensiv zusammengearbeitet habe. Danke für die Unterstützung und die gute Zusammenarbeit.

Zudem möchte ich allen anderen Kollegen danken, die mir im Laufe meiner Masterarbeit bei diversen Gelegenheiten mit Rat und Tat zur Seite gestanden sind.

Ganz besonders möchte ich meinen Eltern danken. Vielen Dank dafür, dass ihr mich während meines Studiums immer unterstützt habt.

Abstract

The aim of the $\bar{\text{H}}$ -HFS experiment of the ASACUSA collaboration is the measurement of the ground state hyperfine splitting of the antihydrogen atom. For that a spin polarized antihydrogen beam will enter a microwave cavity which will induce a spin flip. Afterwards a superconducting sextupole magnet will be used to select a spin. In the end our antihydrogen detector will be used to detect these antiatoms .

It is planned to use a cooled polarized atomic hydrogen beam line to test the cavity and the superconducting magnet. Since a high background of hydrogen is expected, it is necessary to process the data appropriately. Therefore a tuning-fork chopper will be used to produce a bunched hydrogen beam. Afterwards it is possible to remove the noise with a software based lock-in amplifier, which is the subject of this thesis.

Das Ziel des $\bar{\text{H}}$ -HFS Experiments der ASACUSA Kollaboration ist die Messung der Grundzustands-Hyperfeinaufspaltung des Antiwasserstoffatoms. Dafür wird bei einem spinpolarisierten Antiwasserstoffstrahl durch eine Mikrowellenkavität ein Spin-Flip induziert. Danach wird mittels eines supraleitenden Sextupolmagneten ein Spin ausgewählt. Schlussendlich wird ein Antiwasserstoff-Detektor verwendet, um diese Antiatome zu detektieren.

Es ist geplant einen gekühlten und polarisierten atomaren Wasserstoffstrahl zu verwenden, um die Kavität und den supraleitenden Magneten zu testen. Da ein hoher Hintergrund an Wasserstoff zu erwarten ist, ist es notwendig, die Daten entsprechend zu verarbeiten. Daher wird ein tuning-fork chopper verwendet, um einen gepulsten Wasserstoffstrahl zu erzeugen. Danach ist es möglich das Rauschen mit einem softwarebasiertem Lock-in-Verstärker zu entfernen, was das Thema dieser Arbeit ist.

CONTENTS

1	Motivation	1
1.1	CPT Symmetry	1
1.2	\bar{H} -HFS experiment	2
1.3	Atomic hydrogen beam line	2
1.4	Data acquisition	4
2	Data acquisition theory	5
2.1	Lock in amplifier theory	5
2.2	DAQ Hardware	7
3	Realization of the lock-in amplifier	11
3.1	Signal averaging	11
3.2	Lock in amplifier	12
3.2.1	Lock-in amplifier low pass filter	13
4	Experiments	15
4.1	First lock in amplifier tests	15
4.2	Chopper Tests	17
4.2.1	Chopper monitor function	17
4.2.2	Chopper beat	21
4.3	Lock in amplifier tests	22
4.3.1	Simulations	22
4.3.2	Experimental tests	26
4.3.3	Temporal beam behavior	27
4.3.4	Signal phase shift	28
4.3.5	Inverted Signals	31

5	Discussion and Outlook	35
5.1	Discussion	35
5.2	Outlook	36
	Bibliography	37

CHAPTER 1

MOTIVATION

1.1 CPT SYMMETRY

Symmetries are an important concept in physics. There are three fundamental symmetries in particle physics:

- P-Symmetry is the symmetry under a parity transformation $P(t, \vec{x}) \rightarrow (t, -\vec{x})$
- C-Symmetry is the symmetry under a charge-conjugation transformation $C(p) \rightarrow C(\bar{p})$
- T-Symmetry is the symmetry under a time reversal transformation $T(t, \vec{x}) \rightarrow (-t, \vec{x})$ ¹

It was believed that all of these symmetries are conserved. But in 1956 Lee and Yang showed that parity conservation can be broken in weak processes. [2] This was confirmed experimentally by Wu et al in 1957 [3].

The violation of C symmetry followed theoretically from the violation of P conservation [4], but the combined CP symmetry was thought to be conserved until in 1963 Cronin and Fitch observed a violation in the decays of neutral kaons [5].

In the standard model of particle physics the combination of charge conjugation, parity inversion and time inversion (CPT) is conserved. But there are extensions of the standard model that would allow CPT symmetry violation e.g. as done by Colladay and Kostelecky [6, 7]. Given the fundamental nature of CPT symmetry and the importance of

¹For a more detailed approach to this topic refer to [1].

the standard model in modern particle physics it is a task of particular relevance to search for violations of CPT symmetry. One way to test CPT symmetry is the measurement of the hyperfine structure of antihydrogen ($\bar{\text{H}}$ -HFS).

1.2 $\bar{\text{H}}$ -HFS EXPERIMENT

The 1S ground state hyperfine structure consists of four states with the total spin F and the projection of F on the magnetic field axis M . The states $(F,M) = (1,-1), (1,0)$ are called high field seeking states while the states $(F,M) = (1,1), (0,0)$ are low field seeking states. These names arise from the fact that the former move toward regions with higher magnetic field while the latter move toward weaker field regions.

This behaviour is used to measure the ground state hyperfine splitting of antihydrogen using the Rabi resonance method as in [8]. A cusp trap produces a polarized antihydrogen beam consisting predominantly of low field seekers. Afterwards a microwave cavity is used to induce a spin-flip. If the frequency of the microwaves is equal the Larmor frequency, a spin flip occurs changing the low field seeking state to a high field seeking state. Afterwards a sextupole magnet removes the high field seekers from the beam. In the case of a spin flip, this would lead to a drop in the count rate. Further information on this topic can be found in [9].

1.3 ATOMIC HYDROGEN BEAM LINE

The setup described in section 1.2 has to be tested. Since the production of antihydrogen is rather expensive this tests will be done with hydrogen atoms. For this, a hydrogen beam line has to be built that produces a beam of polarized hydrogen atoms.

This hydrogen beam line was built at the SMI in Vienna in 2013. It consists of several differentially pumped vacuum chambers partitioned by several apertures. These chambers contain a dissociation source to produce hydrogen atoms out of molecular hydrogen, a cryogenic system to cool the beam, two permanent sextupole magnets to polarize the beam, a chopper to bunch the beam and a quadrupole mass spectrometer to detect the atoms. A schematic view of this beam line is shown in figure 1.1. For more information refer to [10].

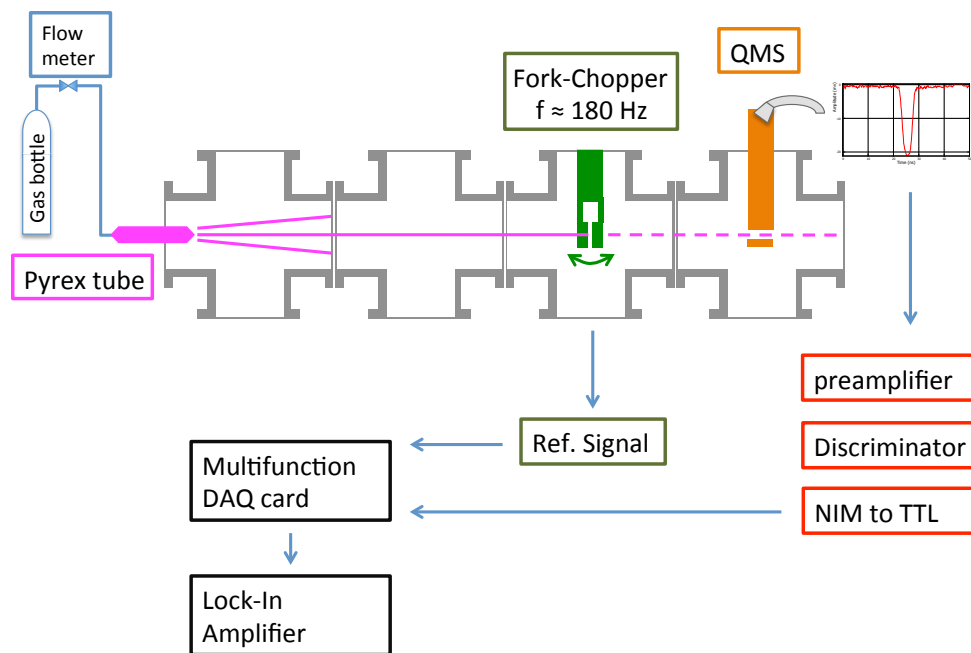


Figure 1.1: Schematic view of the hydrogen beam line, from [10]

1.4 DATA ACQUISITION

This work is largely based on a paper by Walraven and Silvera [11]. As we want to, they built a cooled atomic hydrogen source and used beam modulation techniques to extract the signal from noise and measure the temperature of the beam. To extract the signal a lock-in amplifier was used. Temperature measurement was done using either the phase between signal and reference signal or using the temporal dispersion of the beam. Further details how this is done can be found in the paper.

CHAPTER 2

DATA ACQUISITION THEORY

The goal of the data acquisition is the calculation of the Fourier series of the signal. The Fourier series is a representation of a periodic function as infinite sum of sines and cosines:

$$f(t) = \frac{1}{2}a_0 + \sum_{n=1}^{\infty} a_n \cos(n\omega t) + \sum_{n=1}^{\infty} b_n \sin(n\omega t) \quad (2.1)$$

Since cosines are phase-shifted sines, it is possible to write this equation as

$$f(x) = \frac{1}{2}a_0 + \sum_{n=1}^{\infty} A_n \sin(n\omega t + \phi_n) \quad (2.2)$$

The lock-in amplifier extracts the amplitudes A_n and the phases ϕ_n . A problem is the constant component $\frac{a_0}{2}$ because it can't be calculated by the lock-in amplifier. In our experiment we want to count particles. Negative counts are non-physical so an offset equal to the minimal value of the reconstructed signal is subtracted from the signal.

By integration of this shifted function the number of counts is calculated.

2.1 LOCK IN AMPLIFIER THEORY

A lock in amplifier is in principle a very narrow band pass filter centred around the frequency of a reference signal. Assuming one has a periodic signal of the form

$$A_S \cdot \sin(\omega_S t + \Theta) \quad (2.3)$$

and a reference signal with the same frequency as the signal. A phase locked loop (PLL)

extracts the frequency information of the reference signal and generates a pure sine wave

$$A_R \cdot \sin(\omega_R t) \quad (2.4)$$

This sine wave and the signal with the noise are mixed. Mathematically speaking this is just a multiplication of the signals. For each frequency component in the signal the mixing produces two different outputs.

$$\frac{A_S \cdot A_R}{2} \cos((\omega_S - \omega_R)t + \Theta) + \frac{A_S \cdot A_R}{2} \cos((\omega_S + \omega_R)t + \Theta) \quad (2.5)$$

The only time-independent component of the mixed signal is therefore the first part of this equation for $\omega_S = \omega_R$. Now a low pass filter is used to remove everything except this DC component, leaving in theory only the quantity (with A_R set to 2) $X = A_S \cdot \cos(\Theta)$.

If the mixing is also done with a pure cosine wave, the quantity $Y = A_s \cdot \sin(\Theta)$ is obtained in a similar way. From X and Y it is straightforward to calculate A_S and Θ .

However, in reality it is not possible to remove all the noise since the low pass filter does not remove all AC components. Instead, it attenuates them depending on the selected time constant and filter order with a power rolloff of 20 dB per decade. The time constant τ defines the cut-off frequency via $\omega_c = \tau^{-1}$, while the attenuation is

$$U_o = U_i \cdot \frac{1}{\sqrt{1 + (\omega/\omega_c)^2}} \quad (2.6)$$

with the output/input voltage $U_{o/i}$ for an AC component with circular frequency ω .

By application of more than one low pass filter in series it is possible to increase the filter order. A single low pass filter is called a 1st order filter. Two 1st order low pass filters in series form a 2nd order low pass filter and so on. For higher order filters the attenuation of the high frequency components increase. For a n th order filter the attenuation becomes

$$U_o = U_i \cdot \frac{1}{(1 + (\omega/\omega_c)^2)^{\frac{n}{2}}} \quad (2.7)$$

with a power rolloff of $20 \cdot n$ dB per decade, but on the other hand the settle time, the time it takes for the output to reach and stay within a certain range of the final value, of the filter increases with its order.

2.2 DAQ HARDWARE

As written in the previous section the lock-in amplifier can extract a periodic signal with known frequency. It is therefore necessary to bunch our constant hydrogen beam. This is done with a tuning fork chopper. A tuning fork chopper has a fixed frequency defined by its physical properties. It is driven electro-mechanically in a feedback loop to open and close two vanes. The working principle is as follows: *"Standard drive circuits for tuning fork choppers typically work by taking a signal from a pickup coil on the chopper (usually a slightly distorted sine wave) and amplifying it in a nonlinear manner to produce an approximately square wave drive and reference waveform in phase with the pickup signal."* [14] A picture of this chopper is shown in figure 2.1. The chopper is driven with a 50% duty cycle. What that means is illustrated in figure 2.2.

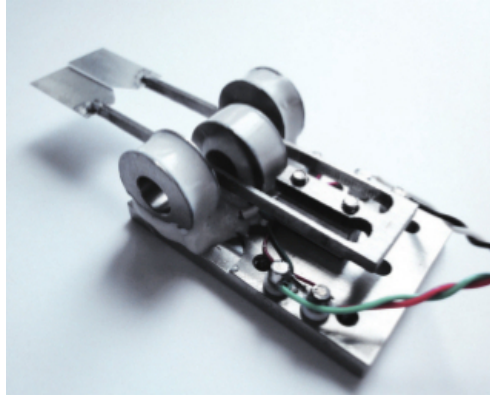


Figure 2.1: Picture of the tuning fork chopper that is used to generate a pulsed beam. The coils generate magnetic fields that move the tines of the fork and thus the attached vanes.

Additionally a driver for the chopper as shown in figure 2.3 was bought. The driver has an adjustable amplitude to manipulate the full opening of the chopper. The monitor output provides a sine wave monitor function to indicate the state of the chopper. Positive half-cycles correspond to an open, negative ones to a closed chopper. The driver can also be used to control two choppers in a master/slave mode with fixed relative phase.

To detect the particles a quadrupole mass spectrometer (QMS) is used. A QMS consists of an ionization source that produces positive ions and a linear Paul trap to analyse the mass-to-charge ratio of the produced ions. Ions that pass through the trap hit an electron multiplier and generate a pulse. A schematic drawing is shown in figure 2.4. More information on QMS can be found in [12].

Normally this type of QMS is used for residual gas analysis, where the ion current is measured, either with a Faraday cup or electron multipliers, and converted into a

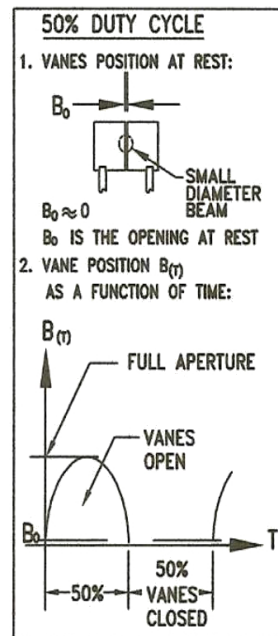


Figure 2.2: the chopper runs with a 50% duty cycle. Point 1 shows the vane position when the chopper is turned off. Point 2 shows the vane position as a function of time when the chopper is turned on. From http://www.eopc.com/ch10_ch20.html



Figure 2.3: Driver of the tuning fork chopper. The amplitude and relative phase between two choppers in a master/slave configuration can be adjusted.

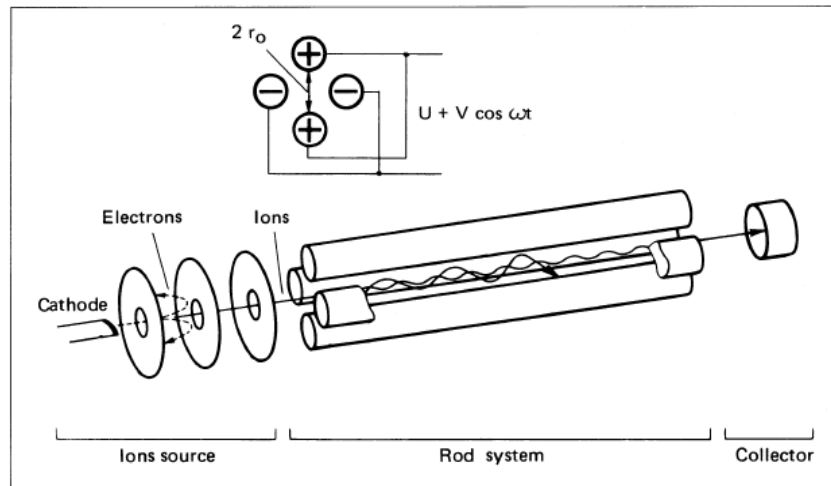


Figure 2.4: Schematic drawing of a QMS, from [13]

pressure. This is not sensitive enough for our experiment so we use single particle detection. Whenever a particle reaches the electron multipliers it generates a negative pulse as in figure 2.5.

Before these pulses can be read by the counter some data processing has to be done. At first the data from the QMS is passed on to a LE1600 leading edge discriminator from GSI. It produces a logical NIM pulse whenever one or more inputs are triggered. To avoid triggering by noise on unused channels their thresholds are set to the maximum of -1 V. Afterwards the NIM pulse is converted to a TTL pulse and sent to the counter.

For data acquisition a NI PCIe-6361 card was used. Since this card has both a counter and an analog input, it is possible to use the same device to acquire the signal and the reference signal. Furthermore the 100 MHz on-board oscillator can be used as a clock, so no external clock is necessary.

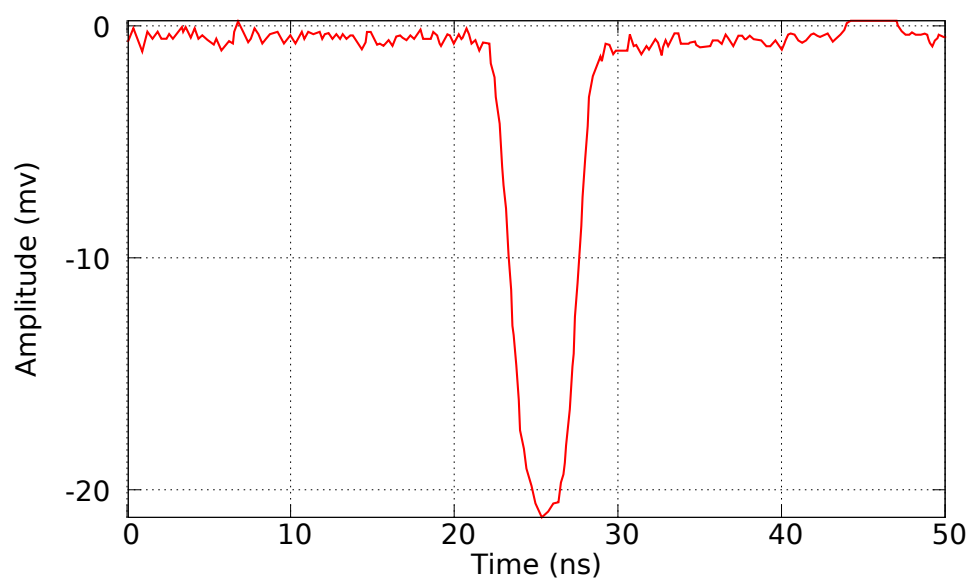


Figure 2.5: QMS output

CHAPTER 3

REALIZATION OF THE LOCK-IN AMPLIFIER

Because of the multitude of apertures in the beam line the expected count rate at the QMS is in the order of several counts per bunch. Such a low count rate makes it impossible to directly apply the lock in amplifier to the signal. So even with the lock in amplifier signal averaging is required. The lock in amplifier then acts on the averaged signal.

3.1 SIGNAL AVERAGING

Signal averaging is done by measuring the minima of the reference sine wave. Then both the reference and the real signal are cut off on these minima. This gives several bunches of data that start and end on minima of the reference sine wave. Remaining data is stored for the next iteration. The reference signal is also averaged because it has to remain a sine wave during averaging. If this is not the case something went wrong with the averaging process. The number of cycles for averaging can be varied between one and sixteen.

More than 16 cycles are not possible at the moment, because the averaging needs the full number of cycles in each iteration. As the rate with which the samples are read out is 10 Hz, one measurement contains slightly less than 18 full cycles, so most of the time a measurement will contain 16 full and two partial cycles what sets the upper limit of 16 cycles.

In principle there are two ways how signal averaging and the lock-in amplifier can be

combined:

One way is to average continuously and send the averaged signal after each iteration into the lock-in amplifier. Since the averaged signal converges to its mean, the same applies for the lock-in amplifier result. With this method averaging over only one cycle is possible but not recommended as the averaged waveforms are strung together to form a continuous waveform for the lock-in amplifier. For averaging over only one cycle random effects in the noise would have the same frequency as the signal itself.

The second method is averaging over a certain period of time or number of iterations. After the averaging is finished, the data is sent into the lock-in amplifier and the averaging restarts. Since this method is much slower and not significantly more accurate it was not implemented.

Depending on the filter settings the lock-in amplifier has a certain settle time. In the calculation of this settle time a continuous signal is assumed. With the frequency of the signal this settle time can be converted into a number of cycles what is more convenient with the signal averaging. The smaller the number of cycles for averaging, the longer it takes for the lock-in amplifier to acquire enough data to settle to its final value.

The number of cycles for averaging also effects the measurement. First the SNR improves with the square root of the number of measurements n . Second, for small count rates, the resolution increases linearly with the number of measurements as $1 + n$. Assuming a signal amplitude in the order of one count without signal averaging the counter will act as 1-bit ADC in regards of the signal, since the number of counts will either be 0 or 1. But each averaging iteration will provide an additional measuring point.

3.2 LOCK IN AMPLIFIER

For the realization of the lock in amplifier the "Lock-In Amplifier Startup Toolkit" from National Instruments was chosen [15]. It has the advantage that it is free and already tested by the company. A drawback is that it is proprietary software an access to the source code is not possible.

In our application the lock-in amplifier itself uses the averaged signal as described in the preceding section to extract the real signal. After each subsequent averaging the new total averaged signal is sent into the lock in amplifier. From this it follows immediately

that the lock-in amplifier will extract the average signal amplitude.

3.2.1 LOCK-IN AMPLIFIER LOW PASS FILTER

The lock-in amplifier offers five different types of filters, two infinite impulse response filters (IIR filters) and three finite impulse response filters (FIR filters). As the name already says the difference between them is their impulse response. For a FIR filter it becomes zero in finite time while for a IIR filter it continues indefinitely. The description of the different filter settings as in the *NILockInStartupKit* manual from [15] are

1. *IIR (2-dig)*

Selects a 10th order IIR filter and displays the time it takes filter to settle to 99 percent of its final value. Numerically, the IIR filter is less expensive than its FIR counterpart, so it can be used to speed-up calculation when time constants smaller than 10,000 x conversion interval are required. It can also be used to reduce filtering overhead when the conversion rate has to be increased. For example, if the conversion rate is 100 kHz, selecting the IIR filter option may allow the application to run on slower computers when filter time constants of 10 ms or less are required.

2. *IIR (5-dig)*

This filter setting is the same as the IIR (2-dig) setting except that the time required for the filter to settle to 99.999 percent of its final value is displayed.

3. *FIR*

Selects 10th order FIR filter. As mentioned previously, this type of filter is more time-consuming than the IIR version for time constants smaller than 10,000 x sampling frequency.

4. *FIR (ENBW)*

This filter setting is the same as the FIR, except that the time constant of the FIR filter is internally modified so that the Equivalent Noise Bandwidth (ENBW) becomes equal to that of the IIR filter with the time constant specified in the TC (s) control. To match the lower noise bandwidth of the IIR filter, the time constant must be increased, resulting in an increased settling time. Although increased, the settling time will

still be shorter than the settling time of the IIR filter if five digits of precision are required.

5. FIR (Sync)

This filter setting is the same as FIR except that the time constant entered into the TC (s) control is coerced to the closest integer multiple of the reference frequency inverse. This is especially useful for smaller reference frequencies where the $(\omega_R + \omega_S)$ frequency component generated by the mixer can be very close to the DC component. For example, if the reference frequency is $f_R = 0.1$ Hz, the mixer will produce the desired DC signal as well as an unwanted frequency component at $2f_R = 0.2$ Hz. It is the task of the low-pass filter to remove the unwanted frequency component. To attenuate this component by 60 dB, using a 4th order IIR filter would require at least 50 or 90 seconds to settle to five digits. The FIR filter, however, has poles located at the integer multiples of $1/TC$ Hz and accomplishes this much faster. For example, a 3rd order sync-FIR filter will attenuate the $2f_R$ component to more than 60 dB and completely settle in 30 seconds if its time constants are within 0.9 to 1.1 of the $1/(2 f_R)$. If the sync window can be calculated more precisely this time can be reduced to 20 seconds or less.

For modern computers the calculation speed is no problem so we can use the FIR filters without problems. Compared to the FIR (ENBW) filter the FIR filter allows a better control over the time constant and therefore the settling time. To chose between the FIR and the FIR (Sync) filter one has to look on the $(\omega_R + \omega_S)$ frequency component. With 180 Hz it will be way off the DC component so it is convenient to use the normal FIR filter.

CHAPTER 4

EXPERIMENTS

4.1 FIRST LOCK IN AMPLIFIER TESTS

First tests of the lock-in amplifier were done with a LED and a photo diode. The LED was driven with a square pulse that would also act as reference signal for the lock-in amplifier. This should test two things:

- Can the lock-in amplifier reconstruct the correct signal?
- Can the lock-in amplifier extract the signal from noise?

For the first point the experimental setup was shielded to avoid noise on the signal. The lock-in amplifier would act on a very clear signal. As shown in figure 4.1 it was capable of reconstructing the signal. Note that the lock-in amplifier result is centred around zero because the lock-in amplifier removed the DC component of the signal.

For the second point noise was added to the signal. A constant offset and 50 Hz periodic noise came from a neon lamp on the ceiling, while random noise was produced with a laser pointer. To get a worse SNR the signal amplitude was decreased in this measurement. The measurement is shown in figure 4.2. The red signal is so noisy that it is impossible to see the underlying periodic signal.

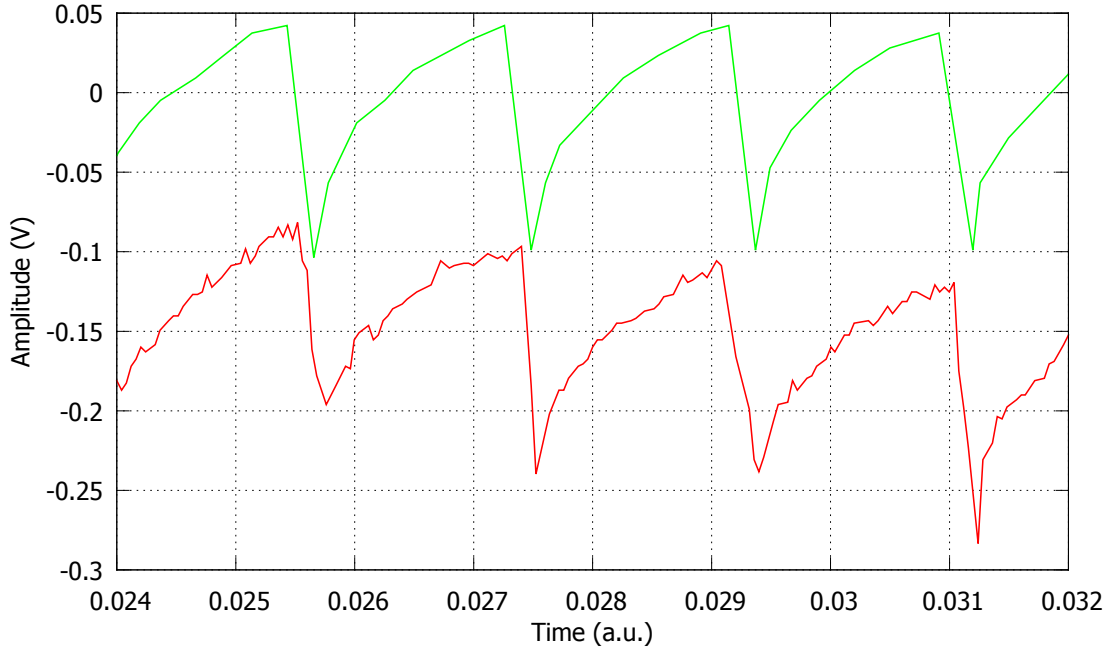


Figure 4.1: A first test of the lock-in amplifier with a LED and a photo diode. Red: real signal, Green: lock-in amplifier result.

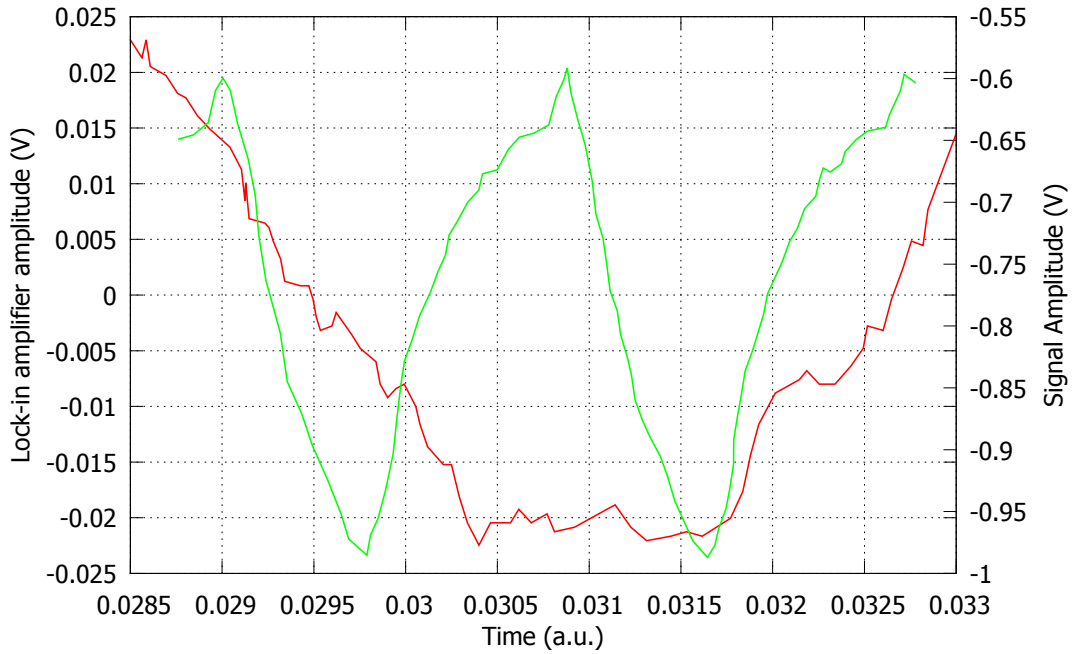


Figure 4.2: A first test of the lock-in amplifier with a LED and a photo diode. Red: real signal, Green: lock-in amplifier result. Noise on the signal comes from surrounding light and a laser pointer

4.2 CHOPPER TESTS

4.2.1 CHOPPER MONITOR FUNCTION

Before the chopper was installed in the beam line first measurements of the chopper monitor function were done. As mentioned in section 3.1 signal averaging requires a stable frequency. It was therefore necessary to measure the frequency stability of the tuning fork choppers to verify that they fulfil the requirements.

FREQUENCY STABILITY

As shown in figure 4.3 the frequency of the chopper monitor function changes with the selected amplitude. Although this was not expected, this is no problem as long as the frequency is stable for a selected amplitude.

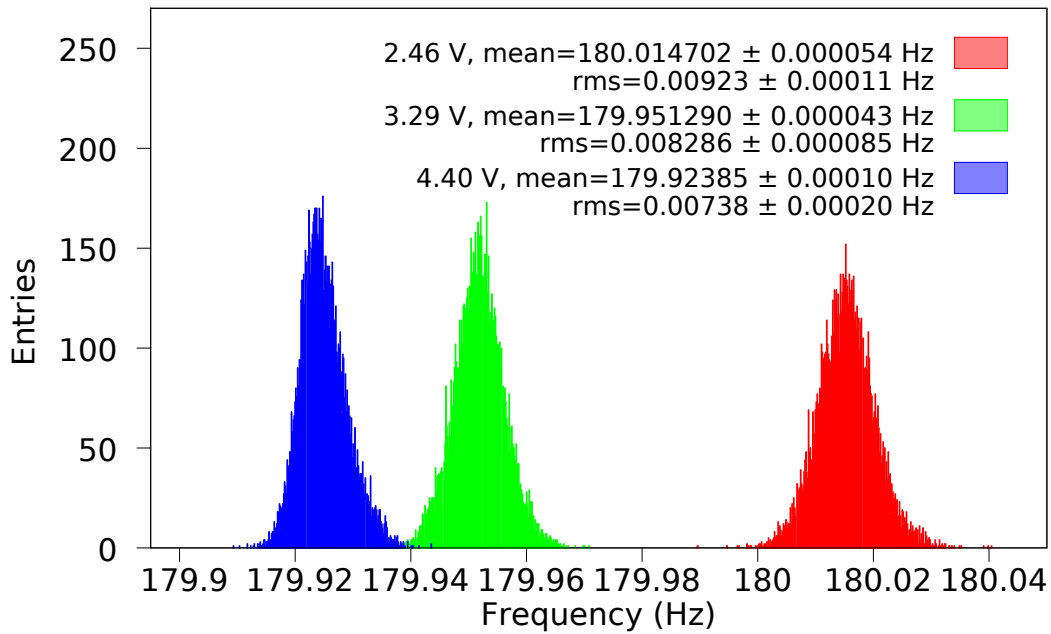


Figure 4.3: Chopper monitor function frequency for different amplitudes. An increase in amplitude clearly decreases the frequency.

A 16.25 hour measurement of the chopper monitor function with a constant amplitude shown in figure 4.4 indicated that the frequency is also not stable in time.

With a sampling frequency of 100 kHz the detected frequency decrease from 179.4 Hz to 178.9 Hz is equivalent to a increase in the cycle length of two samples, or 0.12 samples per hour. Since the usual measurement time is expected to be at maximum in the order of

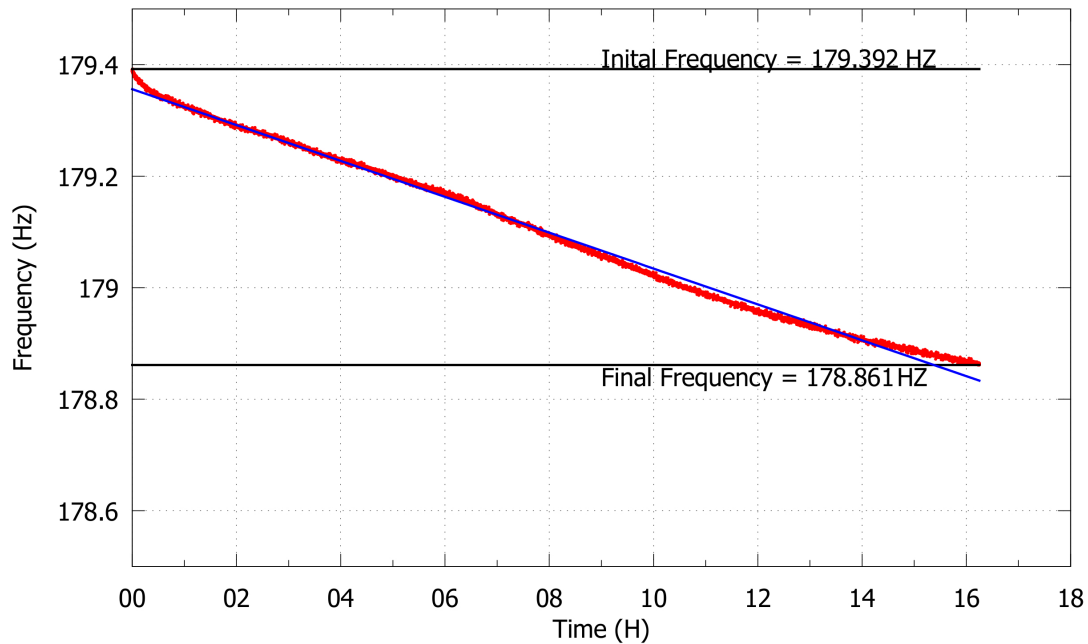


Figure 4.4: Development of the frequency of the chopper monitor function in time. The decrease is 0.3 % in 16.25 hours.

minutes this can be neglected.

A second measurement some weeks later shown in figure 4.5 indicated that this decrease was gone.

Nevertheless, this unexpected behaviour lead to a request to the manufacturer. According to the manufacturer the choppers have to go through an aging process that takes several month before the chopper frequency becomes stable.

HIGH FREQUENCY NOISE

High frequency noise occurred on the chopper monitor function as shown in figure 4.6(a) on the following occasions:

- the hydrogen source is turned on
- a power cable is plugged in
- randomly

This is a problem because the valley detection of the reference signal can't work with the noisy signal. Since the chopper is in a feedback loop, it is unclear if there are other,

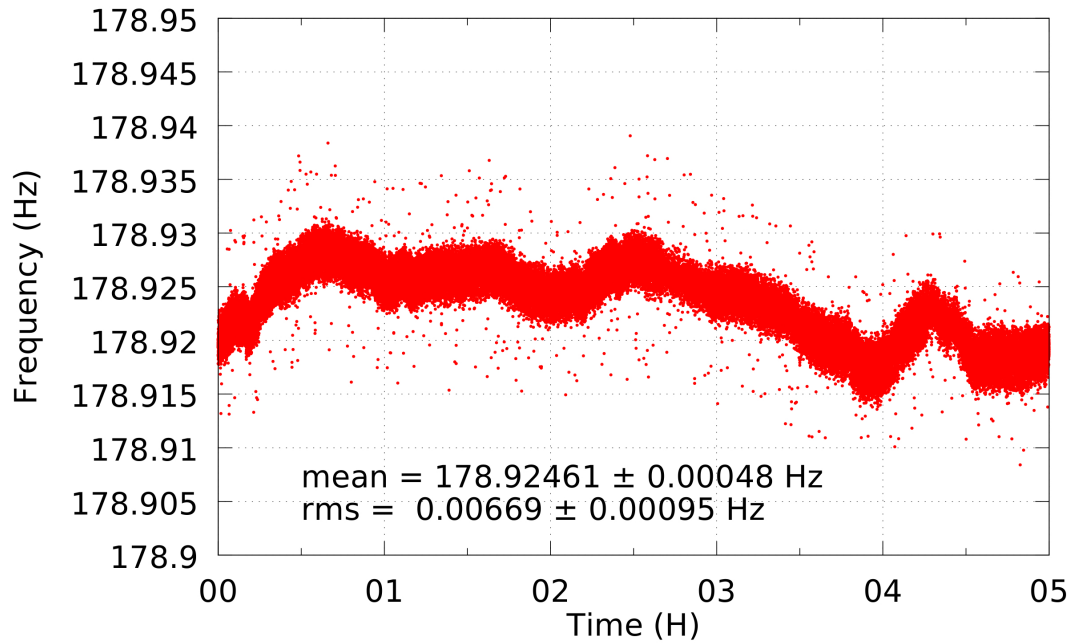


Figure 4.5: A seconds measurement of the development of the frequency of the chopper monitor function in time. Beside small fluctuations the frequency is now stable.

especially mechanical effects of this noise. It is recommended to remove the noise from the signal before a new measurement is started. This can be done by disconnecting the signal cable from the chopper driver.

However, a low pass filter allows it to continue a running measurement if the noise occurs. Such a filter with 20 kHz cut-off frequency was implemented. With that cut-off frequency enough noise is attenuated while the phase shift of the reference signal remains negligible. Figure 4.6(a) shows the noise and figure 4.6(b) the signal after the low-pass filter. Although not all the noise is removed the filtered signal has a much better shape in the valleys what is important for the valley detection algorithm. The remaining noise is removed in the averaging of the reference signal as shown in figure 4.6(c).

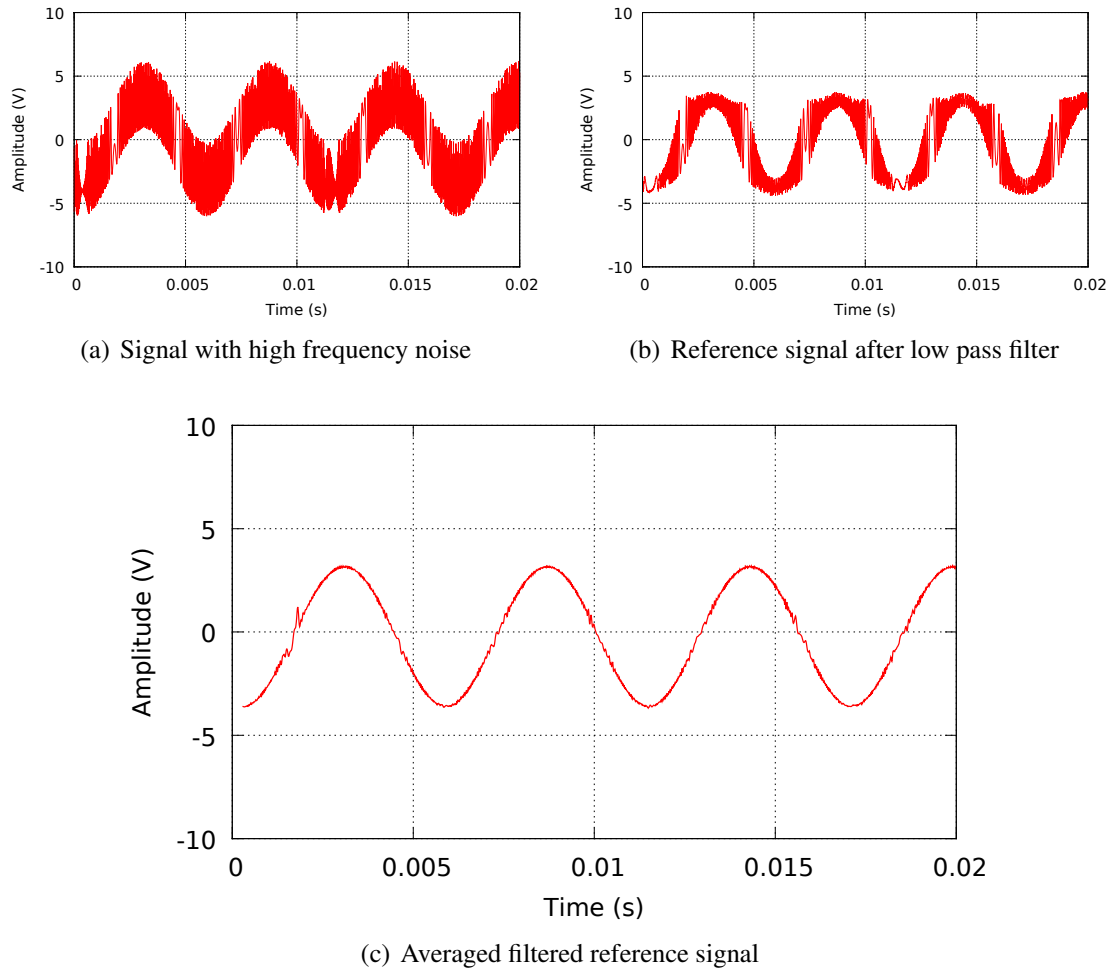


Figure 4.6: High frequency noise on the chopper monitor function before (a) and after (b) a low-pass filter. Averaging of (b) leads to the signal in (c) that is used to calculate the frequency of the reference signal.

4.2.2 CHOPPER BEAT

Another problem if two choppers are connected to the driver is a beat on the choppers. This beat probably originates from distortions in the chopper monitor function as one can see in the FFT of the chopper monitor function in figure 4.7. The distortions in the slave chopper monitor function are much stronger as is the beat on the slave chopper. In a small region between 3.5 to 4 V amplitude the distortions in the monitor function and the beat suddenly vanish (FFT in figure 4.8), while for amplitudes above 4 V things get even worse: The chopper blades of chopper A start to hit each other. Since this might lead to damages of the chopper no measurement of the FFT was done with such an amplitude. Changes in the relative phase between the choppers had no effect on the problem.

If only one chopper is connected to the driver the FFT of the chopper monitor function looks like in figure 4.8, but at high amplitudes the chopper blades still start to hit each other.

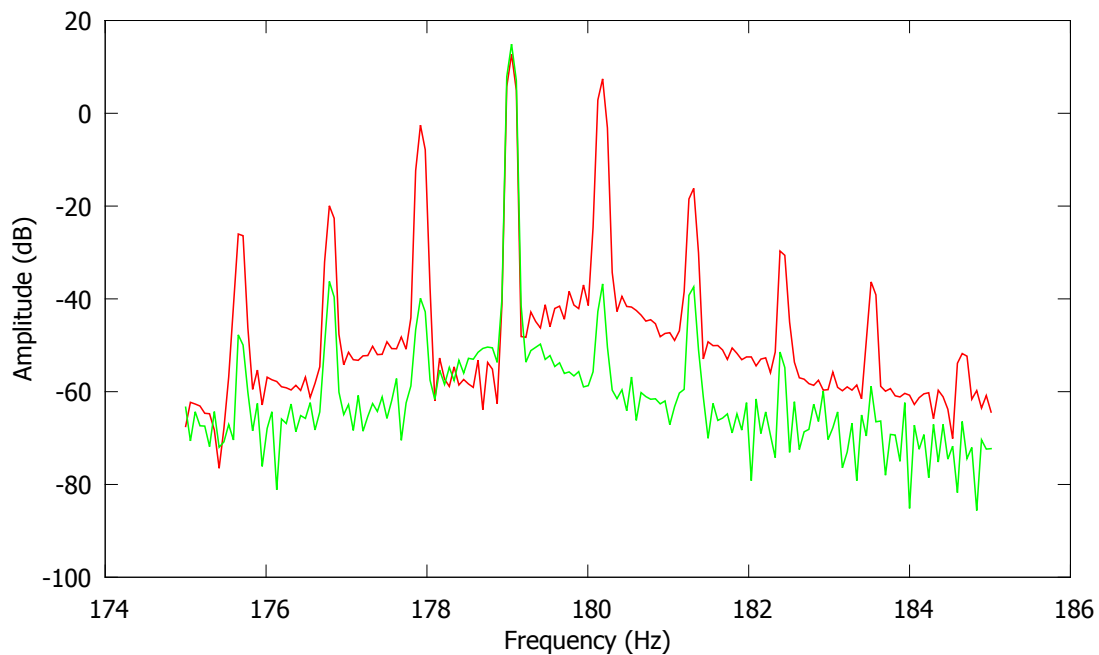


Figure 4.7: FFT of the chopper monitor functions with an amplitude of 1.6 V. Green: Chopper A (Master), Red: Chopper B (Slave).

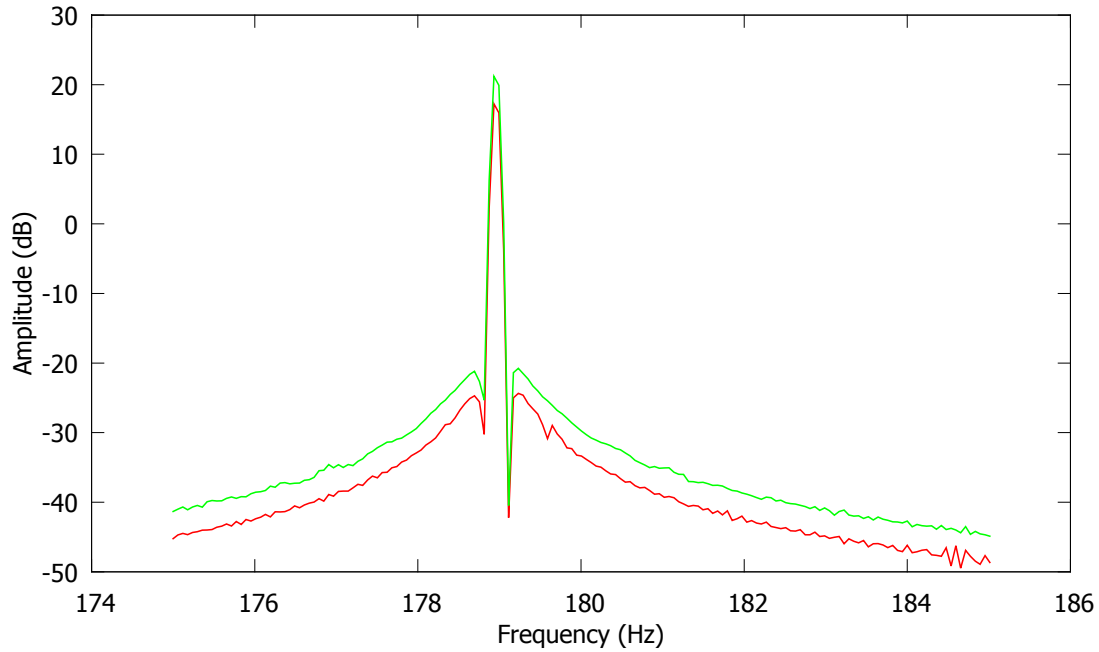


Figure 4.8: FFT of the chopper monitor functions with an amplitude of 3.9 V. Green: Chopper A (Master), Red: Chopper B (Slave).

4.3 LOCK IN AMPLIFIER TESTS

4.3.1 SIMULATIONS

Simulations were done using an artificial periodic signal with a constant offset and random white noise. Since the counting of particles is a poisson process, the amplitude of the white noise was chosen as the square root of the offset to match the experimental conditions. Since the frequency of the choppers is not constant a frequency of 178.35 Hz was selected what is near the expected frequency of the chopper.

Figure 4.9(a) shows beside the expected statistical error also a systematic error proportional to the background. In principle a systematic error from the offset is no surprise. During the mixing the DC component is shifted to the signal frequency. The attenuation for this frequency component would follow from equation 2.6.

But when doing the calculations the attenuation of this noise does not fit the measurement. Moreover this systematic error also occurred for different filter settings with the same slope. The reason for this systematic error couldn't be found, but as a solution a background correction was implemented before the lock-in amplifier. The mean value of the averaged

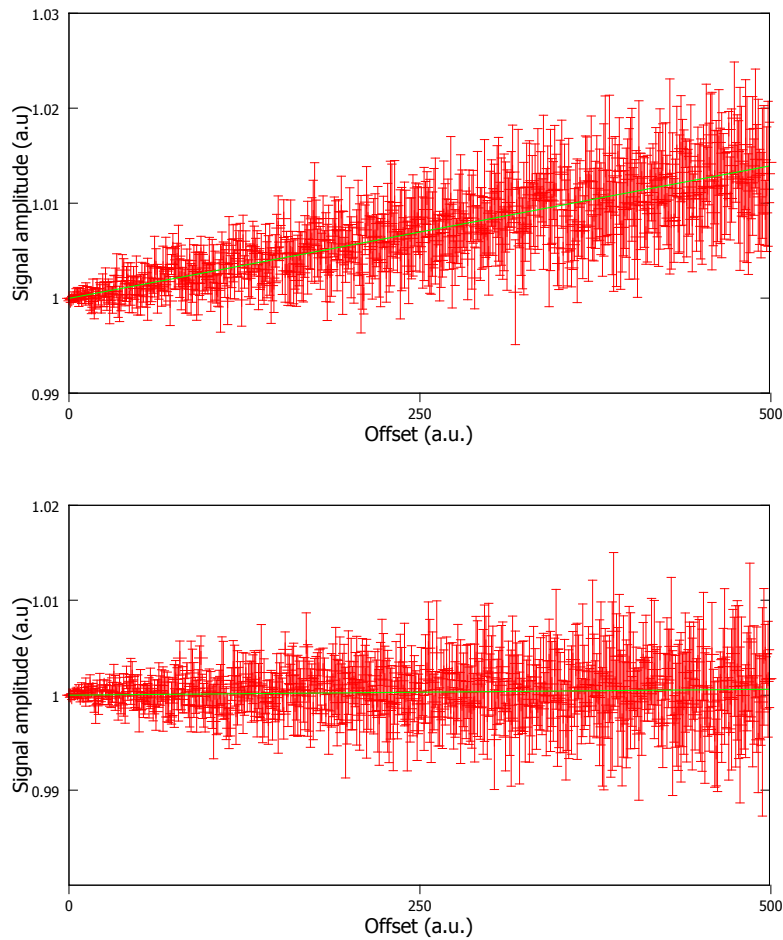


Figure 4.9: Top: 1st order FIR filter with time constant of 1 second acting on a pure sine wave mixed with noise, Bottom: the same measurement preceded by background correction. The offset is n times the signal amplitude.

signal is subtracted before it is sent into the lock-in amplifier. As shown in figure 4.9(b) this resolves the problem.

Surprisingly the filter settings had no influence on the accuracy of the measurement. The figures 4.10 and 4.11 show four tests with the same averaging time but different filter settings. There is no difference in the results.

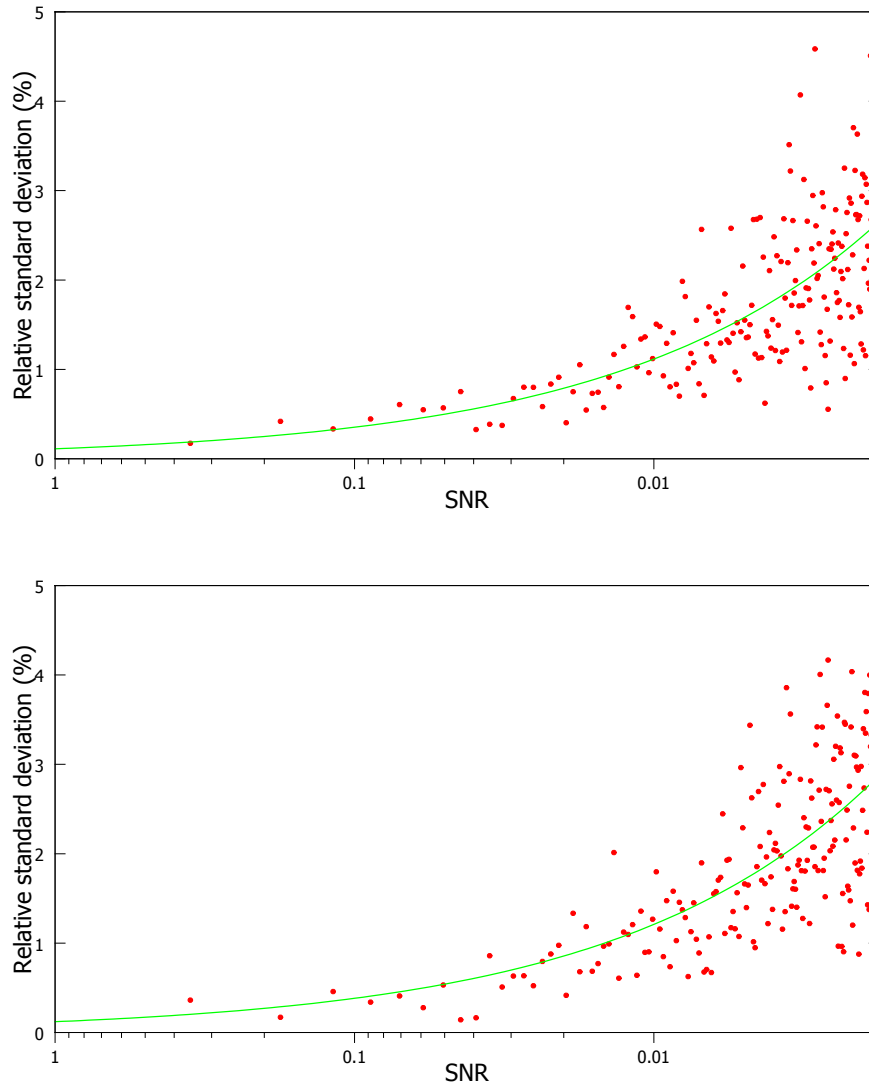


Figure 4.10: Top: Simulation of a FIR filter with 10 seconds of averaging, a time constant of 1 second and filter order 1. Bottom: The same measurement with a time constant of 10 seconds. The SNR in the plots already take the improvement of \sqrt{n} through signal averaging into account.

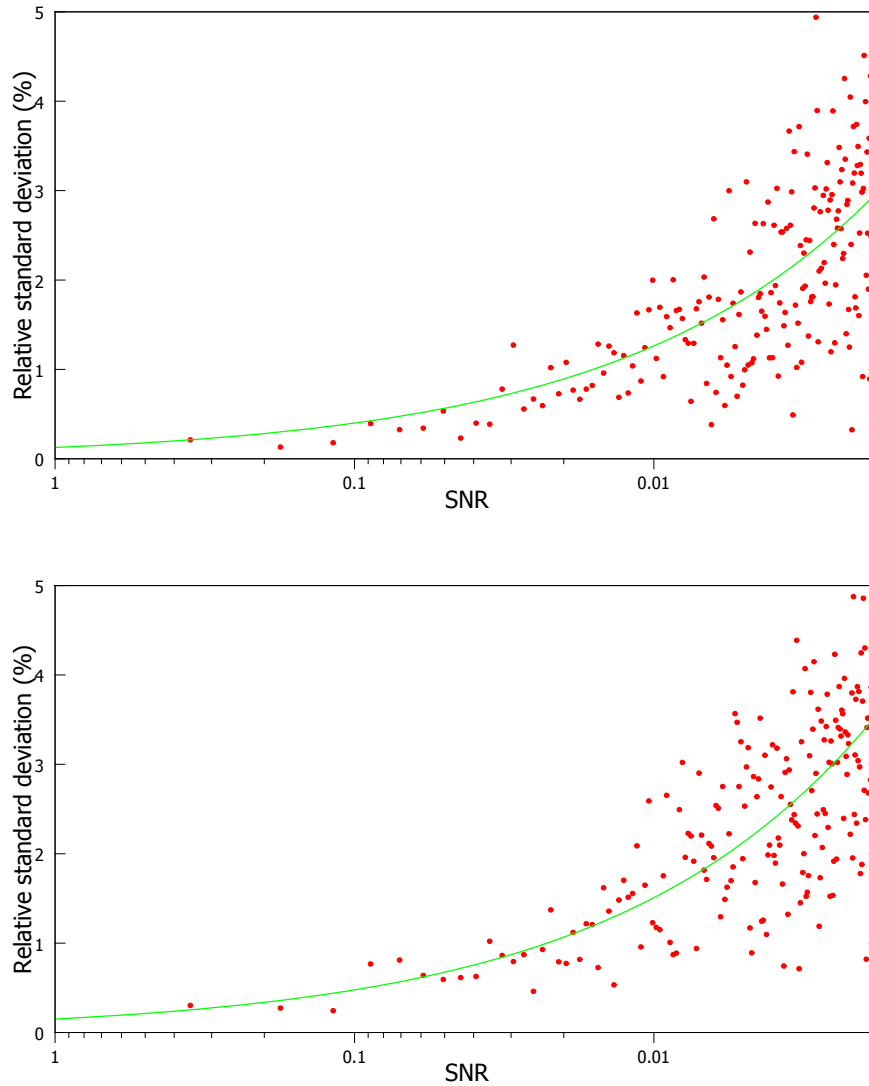


Figure 4.11: Top: Simulation of a FIR filter with 10 seconds of averaging, a time constant of 1 second and filter order 10. Bottom: The same measurement with a time constant of 10 seconds. The SNR in the plots already take the improvement of \sqrt{n} through signal averaging into account.

4.3.2 EXPERIMENTAL TESTS

Beside the simulations also tests with the real beam were done. These tests included tests of the averaging, tests to which order one has to measure for a good signal reconstruction and tests of the lock-in amplifier.

FOURIER SERIES ORDER

For a good signal reconstruction it is crucial to measure up to the right harmonic order of the Fourier series. If the order is chosen to low, information is lost. On the other hand if the order is too high it will not add information but noise to the result. In general the order should be in the range from five to ten, but it is better to determine the exact number by a simple measurement. This is done the following way: One takes a series of measurements with same conditions and calculates the standard deviations of the phases. If the standard deviation is larger than 1 rad the scattering of the measured phases is not better than the scattering of random phases.

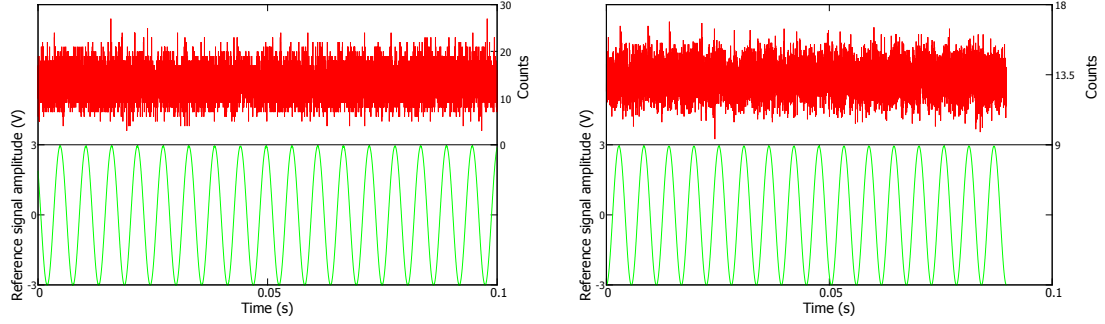
An example is given in table 4.1, that shows a typical lock-in amplifier measurement of a H₂ beam. Beginning with order 7 the standard deviation is larger than 1, so the optimal order for measurement is 6.

Table 4.1: Typical result of the lock-in amplifier for a series of five measurements of a molecular hydrogen beam. The measurement contains the fundamental and the terms up to the 9th harmonic, but only the terms up to the sixth harmonic contribute to the signal.

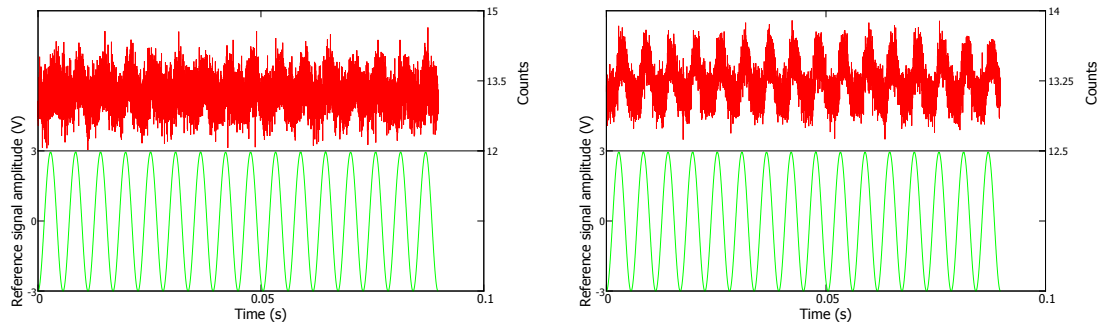
Order	Amplitude (counts)	Phase (rad)
1	0.2556 ± 0.0044	-0.8681 ± 0.0077
2	0.07200 ± 0.0037	-2.855 ± 0.033
3	0.03359 ± 0.0043	-2.71 ± 0.16
4	0.0292 ± 0.0018	1.783 ± 0.075
5	0.0052 ± 0.0032	2.00 ± 0.44
6	0.01449 ± 0.0026	0.34 ± 0.34
7	0.00600 ± 0.0061	-1.3 ± 1.1
8	0.0051 ± 0.0039	-0.6 ± 1.4
9	0.0055 ± 0.0012	0.4 ± 2.3
10	0.0024 ± 0.0015	0.4 ± 2.4

AVERAGING TESTS

Tests of the averaging are straightforward. Since the reference signal is also averaged, it is possible to use it as control function as explained in section 3.1.



(a) Upper part: Real signal as measured with the (b) Upper part: Averaged signal after 1 second. Lower part: Reference Signal. Lower part: Averaged reference Signal after 1 second.



(c) Upper part: Averaged signal after 10 seconds. (d) Upper part: Averaged signal after 60 second. Lower part: Averaged reference Signal after 10 sec- Lower part: Averaged reference Signal after 60 seconds.

Figure 4.12: Effect of averaging on the signal.

The figures 4.12(a) to 4.12(d) give an example of the development of the signal and the reference signal during averaging. As one can see the amplitude and shape of the reference signal stay constant while the SNR of the signal clearly improves.

4.3.3 TEMPORAL BEAM BEHAVIOR

Long time measurements of the count rate of a molecular hydrogen beam showed some kind of sawtooth structure as shown in figure 4.13. This behaviour could be ascribed to temperature changes.

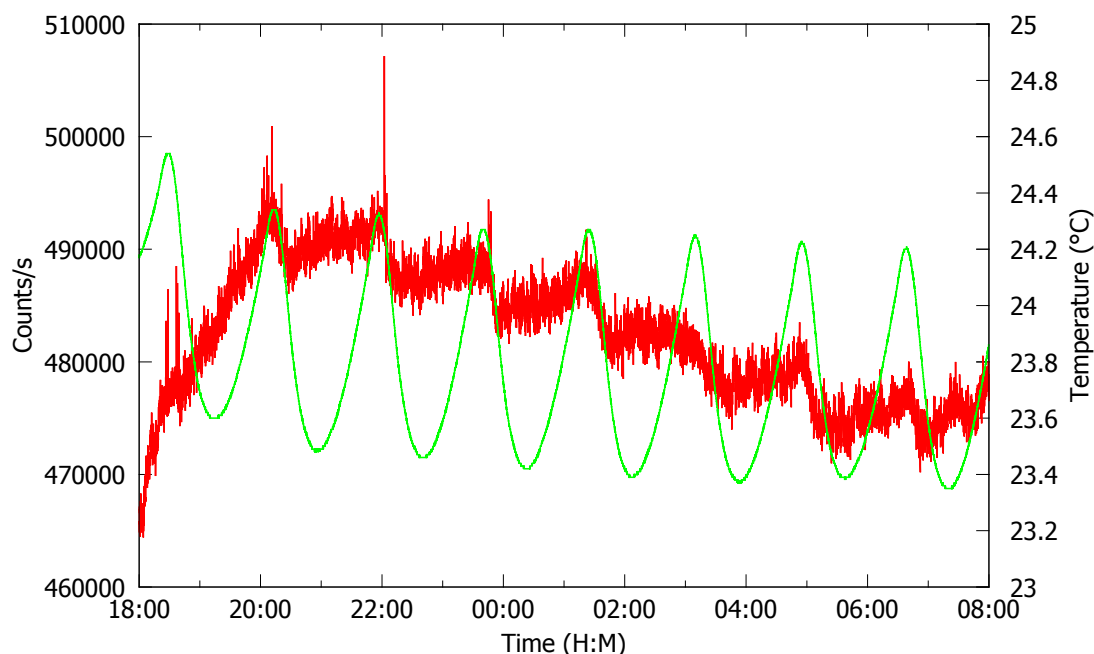


Figure 4.13: Typical measurement of the total count rate (red) and the room temperature (green). The count rate is clearly influenced by the temperature.

TESTS WITH HYDROGEN

First tests of the lock-in amplifier with the beam line were done with molecular hydrogen. Figure 4.14 shows a measurement of the beam with the total counts on top and the lock-in amplifier result on bottom. Although the total signal shows the fluctuations mentioned in section 4.3.3, the result from the beam is stable with a relative standard deviation of 2%.

TESTS WITH ARGON

Later another measurement with argon was done. Argon background arising from the residual gas in the beam line is negligible. This measurement showed a clear dependence of the count rate on the chiller cycle as shown in figure 4.15. This chiller won't be used in the final setup so nothing was done against it.

4.3.4 SIGNAL PHASE SHIFT

During the QMS-optimization measurements it was discovered, that the phase between the chopper monitor function and the detected signal changes significantly during different measurement series. see figure 4.16.

This shift effects the whole signal while the relative phases of the terms of the fourier

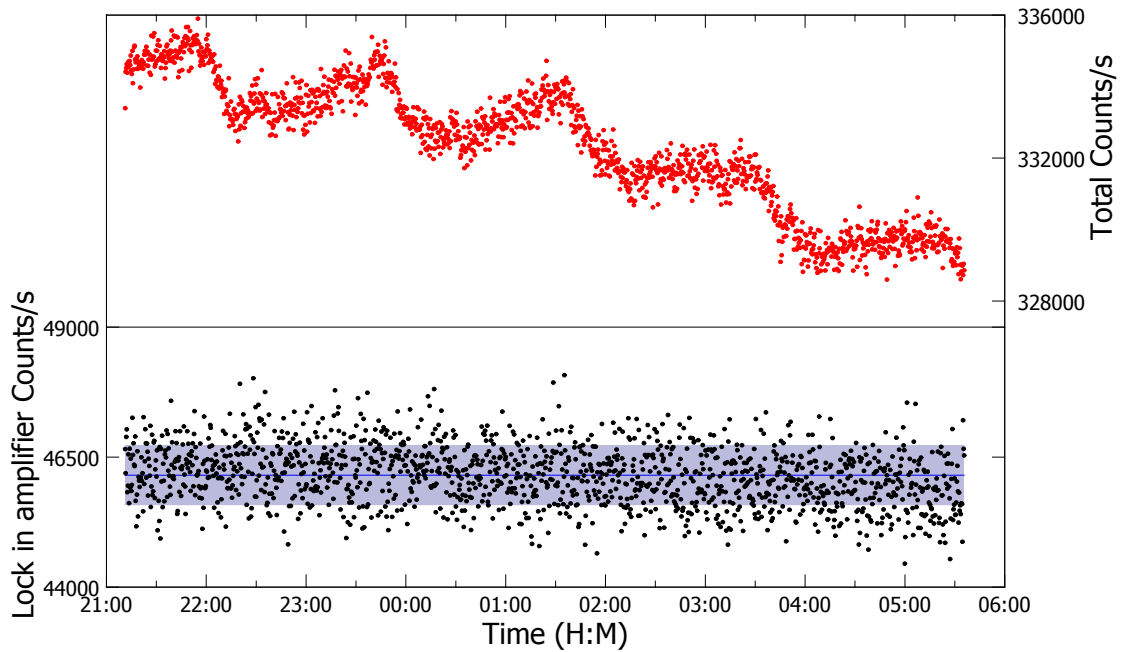


Figure 4.14: On top: Total measured signal. The fluctuations are related to temperature fluctuations. On bottom: Filtered signal using the lock in amplifier. The blue line shows the mean value, the transparent area one standard deviation.

series is stable. This phase shift makes it impossible to determine the beam temperature by measuring the phase difference between the reference signal and the detector signal. For the count rate on the other hand this phase shift makes no difference. A measurement with an oscilloscope directly after the discriminator made it clear that the lock-in amplifier software was the cause of this problem.

The phase shift appears also in the averaged signal, it is therefore not an error in the lock-in amplifier. Within a series of measurements the phase is constant, the problem is therefore at the initialization or the cleanup step. Most likely a buffer is not cleared correctly. If data remains in the buffer it is read out in the next measurement with the new data appended. This would most likely lead to a discontinuity in the signal. This discontinuity would be very distinctive in the reference signal. But there were no discontinuities in the averaged reference signal so the buffer of the counter is not cleared correctly. In principle this discontinuity is also in the data, but there it is buried in noise and not visible.

A explanation could be found in the LabVIEW developer forums: *DAQmx Stop does not clear the aquisition buffer, but you don't really need to worry about that. When DAQmx Start Task is called, the read pointer is set to a new point in the buffer, so when you read*

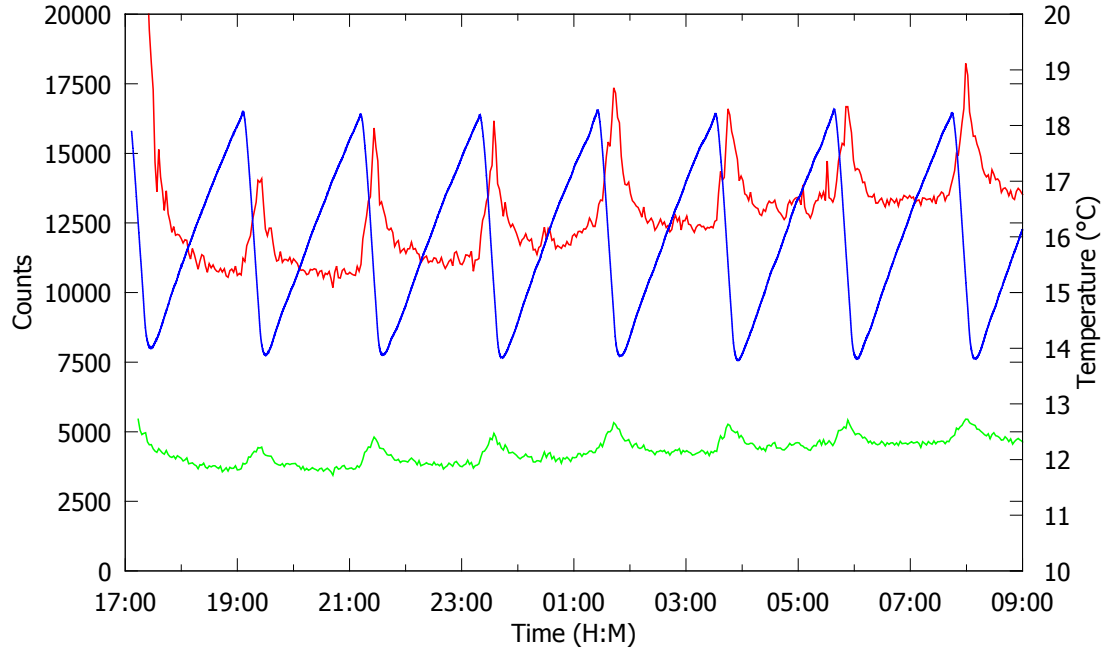


Figure 4.15: Lock in amplifier test with argon. The count rate depends on the chiller cycle. Blue: Chiller temperature, Red: Total counts, Green: Lock-in amplifier result.

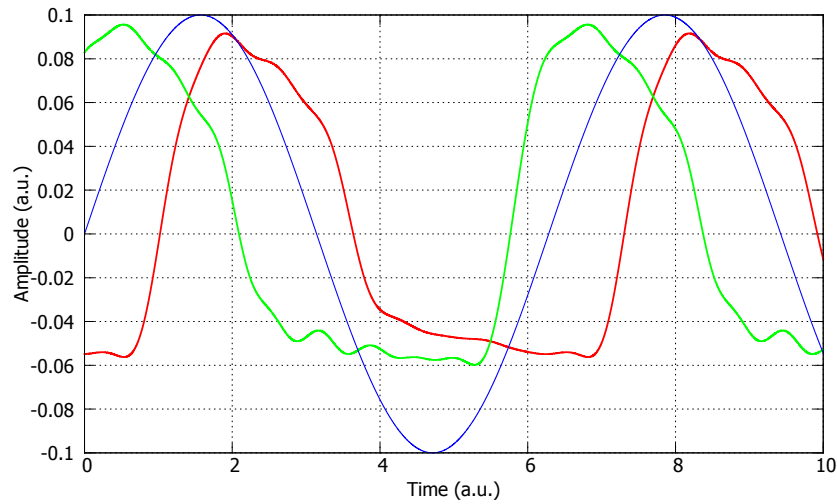


Figure 4.16: The results of the measurements had an unexpected phase shift. The whole signal is shifted both in the lock-in amplifier results and in the averaged data. This lead even to non-physical results as in this plot, where the signal arrived before the chopper was open. Blue: chopper monitor function, Red, Green: Successive measurements of a H_2 beam with same parameters. The red curve was measured first and yields a reasonable result where the particles arrive shortly after the chopper is open. The green curve was measured afterwards and has an unreasonable time delay.

you will only get data from the current iteration of the task.¹ But the type of counting that is used does not use the *DAQmx Start Task*, so the read position is not updated. All the data that was stored after the measurement finished remains in the buffer and is read out during the next measurement. This problem can be resolved by reading out the buffer of the counter before the measurement starts. As shown in figure 4.17 this indeed resolves the phase shift problem.

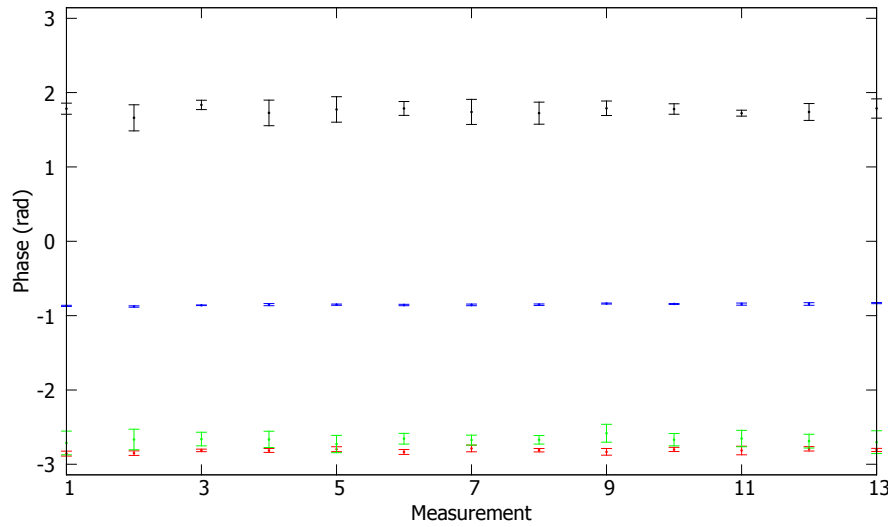


Figure 4.17: Phases of Fourier terms for different measurements. With the buffer readout the phases are constant. Blue: fundamental component, Red: First order harmonic, Green: Second order harmonic, Black: Third order harmonic

4.3.5 INVERTED SIGNALS

Another strange effect that was discovered during the measurements was an inversion of the detected signal as shown in figure 4.18. This effect was observed during the optimization of the QMS and it was soon realized that this effect was somehow related to the count rate. To confirm this two discriminators were used to create a cut out of pulses.

It was clear that this was not a problem of the lock-in amplifier since this effect also appeared in the averaged signal as shown in figure 4.19(a). To find the source of the problem an oscilloscope was used to directly average the logical pulses from the discriminator. As shown in figure 4.19(b) the effect was also visible on the oscilloscope. This problem was therefore related to the hardware.

¹<http://forums.ni.com/t5/Multifunction-DAQ/DAQmx-Stop-Task-Does-executing-this-function-clear-out-the/td-p/1740272>

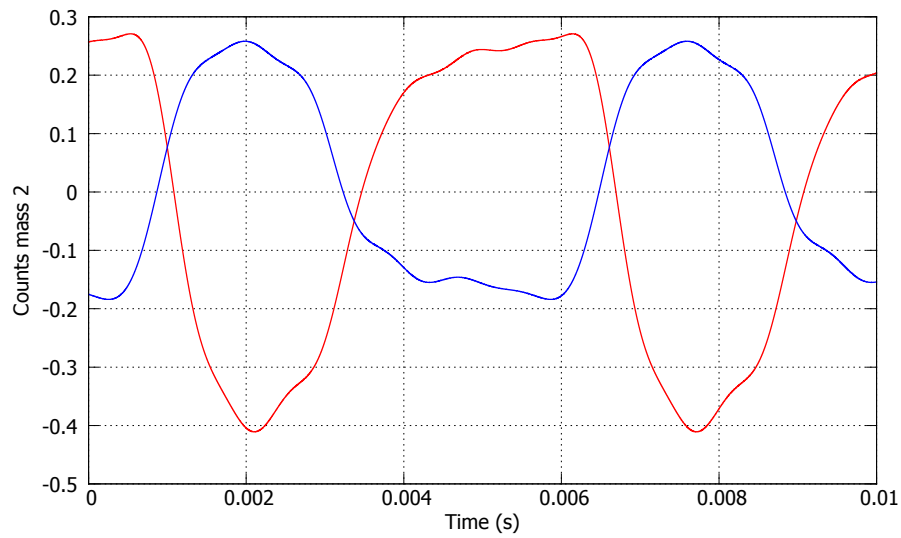
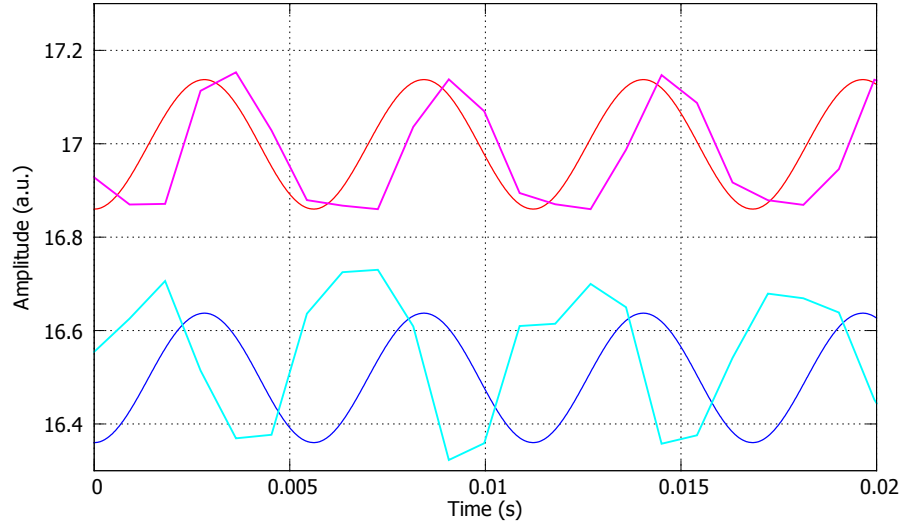
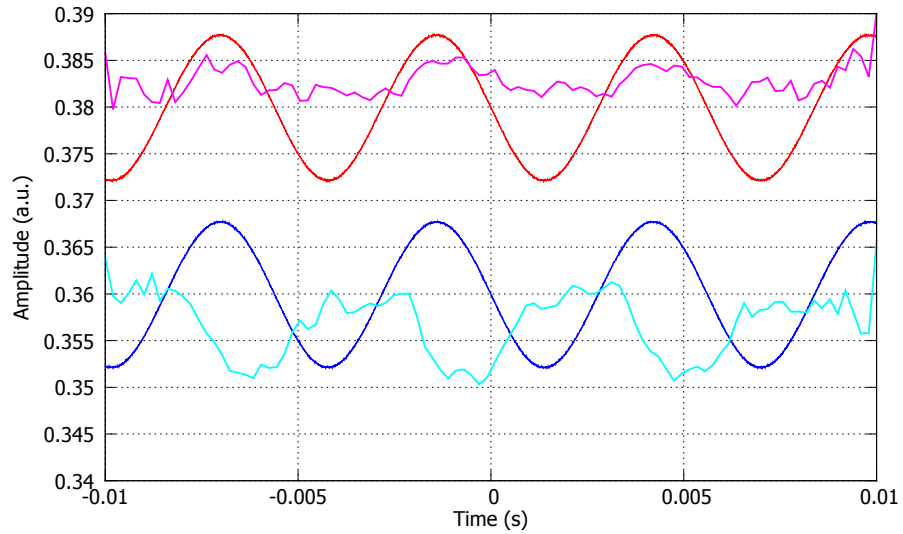


Figure 4.18: Different discriminator settings lead to inverted signals. The red curve has a window of -300 to -350 mV while the blue curve has one of -150 to -200 mV. This leads to different count rates and subsequently to an inverted signal.

Apparently the detection system is paralyzable. At high count rates the discriminator would go into a permanent logical high state and only change to a logical low when there are no counts.



(a) Smoothed averaged signal and chopper monitor function measured with the counter



(b) Smoothed averaged signal and chopper monitor function measured with the oscilloscope

Figure 4.19: Inversion of the measured averaged signal of an molecular hydrogen beam with the software (a) and an oscilloscope (b). To invert the signal the mass was changed from 2.06 (cyan, blue) to 2.09 (magenta, red).

CHAPTER 5

DISCUSSION AND OUTLOOK

5.1 DISCUSSION

In the end the lock-in amplifier worked not as expected but with the desired precision. For the tests of the spin flip cavity and the spin flip analyser magnet the uncertainty of the results has to be smaller than 10%. With the lock-in amplifier this corresponds to a SNR smaller than 10^{-3} after signal averaging.

Because there is no significant improvement for the uncertainty of the result for different filter settings, the only way to decrease the uncertainty is a longer averaging time. Assuming the total background has the same magnitude as in the tests, this is not really a drawback. If the count rate decreases while the total background remains constant, the averaging time has to be increased to maintain a good signal resolution. This will improve the SNR and keep the uncertainty in the desired boundaries of 10%.

A typical result from the tests with atomic hydrogen and an averaging time of 40 seconds was 14094 ± 27 counts/s in total with 4777 ± 40 counts/s from the beam. This means the SNR after averaging was 0.34 and the relative standard deviation of the result was 0.84%.

5.2 OUTLOOK

Since we already reach the desired precision no more work on the lock-in amplifier is planned. Regarding the beam temperature measurements investigation are ongoing. In the meantime the beam line is transported to CERN for the next stage of the experiment. There two permanent sextupole magnets for beam polarization, the spin-flip cavity and the spin flip analyser magnet will be installed. First measurements with atomic hydrogen will be undertaken in 2013.

The planned beam temperature measurements are not implemented yet due to time issues. Very simple measurements using the phase difference between reference signal and the fundamental component of the Fourier series were done and gave results of 500 m/s particle velocities for a molecular hydrogen beam at room temperature, while the theoretical value for the most probable speed is 1560 m/s. It is clear that further research is necessary.

BIBLIOGRAPHY

- [1] D. Schroeder, *Introduction to Quantum Field Theory*. Levant Books, 2005.
- [2] T. D. Lee and C. N. Yang, “Question of parity conservation in weak interactions,” *Phys. Rev.*, vol. 104, pp. 254–258, Oct 1956.
- [3] C. S. Wu, E. Ambler, R. W. Hayward, D. D. Hoppes, and R. P. Hudson, “Experimental test of parity conservation in beta decay,” *Phys. Rev.*, vol. 105, pp. 1413–1415, Feb 1957.
- [4] T. D. Lee, R. Oehme, and C. N. Yang, “Remarks on possible noninvariance under time reversal and charge conjugation,” *Phys. Rev.*, vol. 106, pp. 340–345, Apr 1957.
- [5] J. H. Christenson, J. W. Cronin, V. L. Fitch, and R. Turlay, “Evidence for the 2π decay of the K_2^0 meson,” *Phys. Rev. Lett.*, vol. 13, pp. 138–140, Jul 1964.
- [6] D. Colladay and V. A. Kostelecký, “CPT violation and the standard model,” *Phys. Rev. D*, vol. 55, pp. 6760–6774, Jun 1997.
- [7] D. Colladay and V. A. Kostelecký, “Lorentz-violating extension of the standard model,” *Phys. Rev. D*, vol. 58, p. 116002, Oct 1998.
- [8] I. I. Rabi, S. Millman, P. Kusch, and J. R. Zacharias, “The molecular beam resonance method for measuring nuclear magnetic moments. the magnetic moments of ${}_3\text{Li}^6$, ${}_3\text{Li}^7$ and ${}_9\text{F}^{19}$,” *Phys. Rev.*, vol. 55, pp. 526–535, Mar 1939.
- [9] ASACUSA Collaboration, “Measurement of the antihydrogen hyperfine structure,” *CERN-SPSC 2003-009*, 2003.
- [10] M. Diermaier et al., “Spin polarized atomic hydrogen beam.” To be published in LEAP proceedings 2013.

- [11] J. T. M. Walraven and I. F. Silvera, “Helium-temperature beam source of atomic hydrogen,” *Rev. Sci. Instrum.*, vol. 53/8, p. 1167, 1982.
- [12] E. de Hoffmann and V. Stroobant, *Mass Spectrometry: Principles and Applications*. Wiley, 2007.
- [13] M. Diermaier, “Design and construction of a monoatomic hydrogen beam,” Master’s thesis, Universität Wien, 2012.
- [14] J. Podolske, “Stable sinusoidal driver circuit for tuning fork choppers,” *Review of Scientific Instruments*, vol. 50, pp. 1025 – 1027, Aug 1979.
- [15] National Instruments, “Lock-in amplifier startup toolkit,” http://digital.ni.com/express.nsf/bycode/lockin?opendocument&lang=en&node=seminar_US

LIST OF FIGURES

1.1	Schematic view of the hydrogen beam line, from [10]	3
2.1	Picture of the tuning fork chopper that is used to generate a pulsed beam. The coils generate magnetic fields that move the tines of the fork and thus the attached vanes.	7
2.2	the chopper runs with a 50% duty cycle. Point 1 shows the vane position when the chopper is turned off. Point 2 shows the vane position as a function of time when the chopper is turned on. From http://www.eopc.com/ch10_ch20.html	8
2.3	Driver of the tuning fork chopper. The amplitude and relative phase between two choppers in a master/slave configuration can be adjusted. . .	8
2.4	Schematic drawing of a QMS, from [13]	9
2.5	QMS output	10
4.1	A first test of the lock-in amplifier with a LED and a photo diode. Red: real signal, Green: lock-in amplifier result.	16
4.2	A first test of the lock-in amplifier with a LED and a photo diode. Red: real signal, Green: lock-in amplifier result. Noise on the signal comes from surrounding light and a laser pointer	16
4.3	Chopper monitor function frequency for different amplitudes. An increase in amplitude clearly decreases the frequency.	17
4.4	Development of the frequency of the chopper monitor function in time. The decrease is 0.3 % in 16.25 hours.	18
4.5	A seconds measurement of the development of the frequency of the chopper monitor function in time. Beside small fluctuations the frequency is now stable.	19

4.6	High frequency noise on the chopper monitor function before (a) and after (b) a low-pass filter. Averaging of (b) leads to the signal in (c) that is used to calculate the frequency of the reference signal.	20
4.7	FFT of the chopper monitor functions with an amplitude of 1.6 V. Green: Chopper A (Master), Red: Chopper B (Slave).	21
4.8	FFT of the chopper monitor functions with an amplitude of 3.9 V. Green: Chopper A (Master), Red: Chopper B (Slave).	22
4.9	Top: 1st order FIR filter with time constant of 1 second acting on a pure sine wave mixed with noise, Bottom: the same measurement preceded by background correction. The offset is n times the signal amplitude.	23
4.10	Top: Simulation of a FIR filter with 10 seconds of averaging, a time constant of 1 second and filter order 1. Bottom: The same measurement with a time constant of 10 seconds. The SNR in the plots already take the improvement of \sqrt{n} through signal averaging into account.	24
4.11	Top: Simulation of a FIR filter with 10 seconds of averaging, a time constant of 1 second and filter order 10. Bottom: The same measurement with a time constant of 10 seconds. The SNR in the plots already take the improvement of \sqrt{n} through signal averaging into account.	25
4.12	Effect of averaging on the signal.	27
4.13	Typical measurement of the total count rate (red) and the room temperature (green). The count rate is clearly influenced by the temperature.	28
4.14	On top: Total measured signal. The fluctuations are related to temperature fluctuations. On bottom: Filtered signal using the lock in amplifier. The blue line shows the mean value, the transparent area one standard deviation.	29
4.15	Lock in amplifier test with argon. The count rate depends on the chiller cycle. Blue: Chiller temperature, Red: Total counts, Green: Lock-in amplifier result.	30
4.16	The results of the measurements had an unexpected phase shift. The whole signal is shifted both in the lock-in amplifier results and in the averaged data. This lead even to non-physical results as in this plot, where the signal arrived before the chopper was open. Blue: chopper monitor function, Red, Green: Successive measurements of a H_2 beam with same parameters. The red curve was measured first and yields a reasonable result where the particles arrive shortly after the chopper is open. The green curve was measured afterwards and has an unreasonable time delay.	30

- 4.17 Phases of Fourier terms for different measurements. With the buffer readout the phases are constant. Blue: fundamental component, Red: First order harmonic, Green: Second order harmonic, Black: Third order harmonic 31
- 4.18 Different discriminator settings lead to inverted signals. The red curve has a window of -300 to -350 mV while the blue curve has one of -150 to -200 mV. This leads to different count rates and subsequently to an inverted signal. 32
- 4.19 Inversion of the measured averaged signal of an molecular hydrogen beam with the software (a) and an oscilloscope (b). To invert the signal the mass was changed from 2.06 (cyan, blue) to 2.09 (magenta, red). 33

Michael Wolf
Curriculum Vitae, 2013

CONTACT INFORMATION

Email: Michael.Wolf@assoc.oeaw.ac.at

EDUCATION

2003 - 2007: BORG Mistelbach (Grammar school),

2008 - 2011: Bachelor Degree in Physics, University of Vienna

since 2011: Master Degree in Physics, University of Vienna

2012 - 2013: Master's thesis, Stefan Meyer Institute for Subatomic Physics

CIVILIAN SERVICE

2007-2008, Landespflegeheim Mistelbach - Franziskusheim